Available online at www.CivileJournal.org

Civil Engineering Journal

(E-ISSN: 2476-3055; ISSN: 2676-6957)

Vol. 12, No. 02, February, 2026

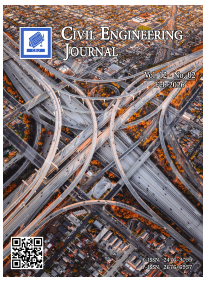

Stiffness Degradation Effects on Seismic Behavior of RC Frame Structures

Phu-Anh-Huy Pham [1, 2*], Tan-Phat Nguyen [2], Ngoc-Han Nguyen [2]

[1] *Institute of Research and Development, Duy Tan University, Da Nang, 550000, Vietnam.*

[2] *Faculty of Civil Engineering, Duy Tan University, Da Nang, 550000, Vietnam.*

Received 10 July 2025; Revised 07 January 2026; Accepted 12 January 2026; Published 01 February 2026

Abstract

This study investigates the influence of stiffness degradation on the seismic performance of reinforced concrete (RC) frame structures, focusing on global response parameters including roof lateral displacement ratio (Δ/H), fundamental period (T_1), and internal force redistribution. Nonlinear finite element analyses were conducted in SAP2000 for three representative RC frames (3-, 10-, and 20-story), considering beam-only, column-only, and combined stiffness degradation scenarios. The analytical framework integrates theoretical derivations of effective stiffness models with response-spectrum-based simulations, following the provisions of Vietnamese code (TCVN 9386:2012) and American code (ACI 318-25), as well as the formulations proposed by Paulay & Priestley, Elwood & Eberhard, and Tran & Li. The results reveal a clear height-dependent and nonlinear relationship between stiffness degradation and seismic response. In low-rise frames, beam stiffness reduction primarily governs lateral deformation, whereas column stiffness degradation dominates the dynamic behavior and internal force concentration in medium- and high-rise systems. When the effective stiffness ratio falls below $EI_d/EI_g = 0.5$, roof drift and fundamental period increase sharply, and internal forces at the column base (M and Q) are amplified, leading to excessive deformation and potential instability. Among the models examined, the Tran & Li formulation provided the highest accuracy and stability when validated against experimental data. The findings emphasize that column stiffness should not be reduced below 50% of the gross section stiffness in high-rise frames to maintain acceptable vibration periods and control lateral drift. The novelty of this work lies in quantifying the nonlinear, height-dependent influence of stiffness degradation across multiple structural parameters, bridging the gap between component-level deterioration and system-level seismic performance. The results provide height-sensitive insights for improving nonlinear seismic analysis and performance-based design of RC frame buildings.

Keywords: RC Frame; Stiffness Degradation; Nonlinear Modeling; SAP2000; Earthquake; Moment; Shear Force; Roof Displacement.

1. Introduction

Reinforced concrete (RC) frames are among the most widely used structural systems in civil and industrial construction, especially for mid- and high-rise buildings. These structures are subjected to both static and dynamic loads, with seismic loads being particularly critical due to their unpredictability and destructive potential. A key factor governing a structure's seismic performance is its stiffness, which characterizes the resistance to deformation and directly influences global responses such as displacement, moment, and shear force [1–3]. When exposed to strong ground motion, RC members, particularly beams and columns, undergo stiffness degradation due to cyclic loading, leading to redistribution of internal forces and displacements, and ultimately affecting the overall stability and safety of

* Corresponding author: phampanhhuy@duytan.edu.vn

https://doi.org/10.28991/CEJ-2026-012-02-011

the building [4, 5]. The primary mechanism of stiffness degradation originates from cracking, reinforcement yielding, bond deterioration, and concrete crushing, which together alter the load–deformation relationship and energy dissipation capacity of the structure. Over the past decades, the seismic performance of RC frames has been a central topic in earthquake engineering research. The devastating impacts of major earthquakes, such as the 1995 Kobe, 2008 Wenchuan, and 2011 Tohoku events, have revealed the vulnerability of RC buildings to stiffness and strength degradation. Even structures designed according to modern seismic codes suffered severe damage or collapse when stiffness loss and force redistribution were not properly accounted for. Consequently, stiffness degradation has become a key indicator of both damage evolution and residual structural capacity during and after seismic events. Numerous design codes (e.g., Vietnamese code TCVN 9386:2012 [6], American codes ASCE 41-22 [7] and ACI 318-25 [8]) and academic models [9-11] have introduced methods for estimating effective stiffness - a parameter that represents the true working stiffness under nonlinear seismic conditions and enables more accurate prediction of inelastic structural responses [12, 13]. Despite these developments, the actual degradation process does not occur uniformly throughout a structure. Beams typically experience early flexural cracking and stiffness reduction, while columns undergo progressive axial–flexural degradation that dominates the global dynamic response. These cumulative effects lead to fundamental period, increased lateral drift, and concentration of internal forces in critical regions such as beam–column joints and column bases. For multi-story frames, the degree and location of stiffness degradation directly influence how lateral forces are distributed across the height, thereby determining the overall seismic behavior and failure mode of the structure.

From a design perspective, most international standards provide empirical stiffness reduction factors derived from single-member tests rather than from system-level evaluations. This simplification, although convenient, often leads engineers to assume homogeneous degradation throughout the structure, which can cause significant errors in estimating key response parameters such as roof drift, fundamental period, and base shear [14–16]. In particular, the interaction between beam and column stiffness degradation remains inadequately addressed, especially in medium- and high-rise RC buildings where column stiffness largely governs lateral resistance. Hence, the validity of existing code-based reduction factors for global seismic analysis is still uncertain. Along with the advancement of computational techniques, nonlinear finite element analysis using programs such as OpenSees [17], ETABS [18], and SAP2000 [19] has made it possible to simulate stiffness degradation with higher precision. By integrating nonlinear constitutive models calibrated with experimental data, these tools can reproduce local cracking and plastic hinge formation, providing more realistic representations of global behavior. However, most previous studies have focused on isolated elements or low-rise frames, whereas comprehensive investigations of multi-story RC frames under varying degradation scenarios remain scarce. Systematic comparisons that assess how stiffness degradation of beams and columns, individually and simultaneously, affects roof displacement, period elongation, base moment, and shear force are still lacking.

Another persistent challenge concerns the selection of appropriate stiffness models for nonlinear seismic analysis. Traditional models by Paulay & Priestley [9] or Elwood & Eberhard [10] are simple and widely used but often neglect the influence of axial load and reinforcement ratios. More recent formulations, such as the model by Tran & Li, incorporate these effects and have shown promising agreement with experimental data, yet their applicability to multi-story structures has not been thoroughly validated. Comparative evaluations of these models at the structural-system level are limited, leaving uncertainty regarding which approach provides the most accurate predictions for practical design and assessment. Concurrently, the philosophy of seismic design has evolved from ensuring elastic behavior toward accepting controlled nonlinear responses, emphasizing the “no collapse” criterion over “no damage.” This paradigm shift highlights the importance of capturing stiffness degradation accurately, as it strongly influences the redistribution of forces, period elongation, and energy dissipation. Khoshraftar & Abbasnia [20] demonstrated that a 50% loss of stiffness or a 40% reduction in strength could lead to significant structural damage. Similarly, Kumar & Singh [21] proposed and experimentally verified a three-component effective stiffness model that improved the correlation between analytical and observed seismic responses. Lima et al. [22], Guo et al. [23], Hamidia et al. [24], and Loh et al. [25] further explored different modeling and experimental techniques, ranging from beam-to-column joint degradation and fractal crack analysis to dynamic identification using the Bouc–Wen model, confirming that stiffness loss is a reliable proxy for damage progression. Nevertheless, the combined impact of beam and column stiffness degradation on the overall dynamic performance of RC frames across different building heights has not been systematically quantified. The lack of such data constrains the reliability of nonlinear seismic analyses and limits the development of height-sensitive design recommendations. Therefore, a comprehensive investigation linking component-level stiffness models to system-level seismic behavior is necessary to enhance both analytical accuracy and design safety.

In this study, a systematic framework is established to evaluate the influence of stiffness degradation on the seismic behavior of RC frame structures. Nonlinear response-spectrum analyses are performed using the Finite Elemnent Method (FEM) on three representative RC frame configurations (3-, 10-, and 20-story), incorporating beam-only, column-only, and combined degradation scenarios. The effective stiffness models are selected from both international design codes (TCVN 9386:2012, ACI 318-25) and previous academic formulations [9-11]. By comparing analytical

predictions with available experimental data, the study identifies the most reliable and stable stiffness model for practical seismic assessment. The findings clarify how degradation mechanisms scale with building height and how they influence critical response parameters such as displacement, period, and internal forces. The novelty of this research lies in bridging the gap between component-based degradation models and system-level seismic performance, thereby improving the realism and reliability of nonlinear seismic design for RC frame structures. The remainder of this paper is organized as follows: Section 2 describes the research methodology, including the theoretical basis for stiffness modeling and the simulation framework. Section 3 presents and discusses the numerical results, highlighting the effects of stiffness degradation across different frame heights. Section 4 concludes with key findings, limitations, and recommendations for future research.

2. Research Methodology

The research methodology of this study consists of two main components: theoretical analysis and numerical simulation. Specifically, the theoretical approach establishes a solid foundation for determining stiffness, stiffness degradation, and effective stiffness of RC structures under seismic loading. Subsequently, the numerical simulation is conducted using the FEM (through SAP2000 – version 26 [19]) to model the seismic response of RC frames with varying numbers of stories.

2.1. Stiffness Theory

The theoretical framework relies on fundamental concepts of stiffness and effective stiffness as applied to structural behavior under seismic loads. In this context, structural stiffness is defined as the ability of a structural member (beam or column) to resist deformation under external forces. Stiffness may vary over time, particularly under the influence of seismic loading, leading to stiffness degradation. Stiffness can be categorized into three main types:

- Initial stiffness: the slope of the force–displacement curve in the elastic range, representing the structure's resistance to deformation under elastic loading conditions.
- Secant stiffness: the slope of a straight line connecting the origin to a specific point on the force–displacement curve, used to describe structural behavior under various loading levels.
- Tangent stiffness: the slope of the tangent line to the force–displacement curve at a given point, representing structural behavior beyond the elastic limit under large deformations.

In addition, effective stiffness is a critical factor in seismic design and is calculated based on several empirical and code-based models. These include those proposed by scholars such as Elwood & Eberhard [10], Paulay & Priestley [9], and design codes (ACI 318-25 [8] and ASCE 41-22 [7]). Effective stiffness accounts for the reduction in stiffness due to cracking and the variation of material properties, especially when structural members are subjected to seismic loading.

2.2. Numerical Simulation Method

2.2.1. RC Frame Modeling

The RC frame models were developed with three different configurations of three-bay frames, each varying in the number of stories: a 3-bay, 3-story frame (3B-3S) representing low-rise buildings; a 3-bay, 10-story frame (3B-10S) representing mid-rise buildings; and a 3-bay, 20-story frame (3B-20S) representing high-rise buildings. Structural parameters, including the cross-sectional dimensions of columns and beams, material elastic moduli, and boundary conditions, were defined in accordance with current design standards (TCVN 9386:2012 [6] and ACI 318-25 [8]). All frame systems were assumed to be subjected to seismic loads, analyzed using the response spectrum method.

2.2.2. Seismic Analysis Using Response Spectrum Method

The response spectrum method was employed to evaluate the seismic behavior of the RC frame structures. In this method, earthquake input is modeled using a ground acceleration spectrum, enabling the calculation of structural responses across a range of vibration frequencies. Key response parameters such as displacement, moment, and shear force at critical structural locations are then obtained. In this study, ground acceleration spectra were developed based on the seismic characteristics of the considered site, including peak ground acceleration and frequency content. These spectra were then applied in SAP2000 software to simulate and analyze the seismic responses of the frame systems under various scenarios. In the response spectrum analyses, a constant critical damping ratio of 5% was adopted for all frame models (3-, 10-, and 20-story). This value is recommended by both TCVN 9386:2012 [6] and ACI 318-25 [8] for reinforced concrete structures subjected to seismic loading, and is widely accepted in seismic design practice. Using a uniform damping ratio ensures consistency across the three models and allows for direct comparison of their seismic responses.

2.2.3. Analysis Parameters

The key parameters analyzed in this study include:

- Roof lateral displacement (Δ): this parameter reflects the horizontal displacement of the frame's roof under seismic excitation and is directly related to the overall stability of the structure.
- Fundamental period (T_1): T_1 represents the natural period of the structure's first mode of vibration and indicates the flexibility or stiffness of the system. A longer T_1 suggests a more flexible structure with greater deformation tendencies, whereas a shorter T_1 indicates a stiffer system with better displacement resistance. T_1 is strongly correlated with the seismic demand imposed on the structure through the response spectrum.
- Column base moment (M): the maximum calculated moment at the column base, representing a critical index for evaluating the column's load-bearing capacity under seismic forces.
- Column base shear (Q): the maximum shear force at the base of columns, serving as a crucial indicator of internal force distribution and the structure's lateral load-resisting performance.

All of the above parameters were calculated and assessed through simulations performed in SAP2000, thereby providing insights into the seismic behavior of RC frame structures subjected to stiffness degradation.

2.3. Numerical Simulation Method

Effective stiffness is a critical criterion for structural analysis under seismic loading. The lateral stiffness (K) of a structural member subjected to double curvature bending can be calculated using Equation 1. Paulay & Priestley [9] proposed values for the effective moment of inertia of beams and columns based on the axial load ratio, as shown in Table 1.

$$K = 12EI/L^3 \tag{1}$$

where E is the elastic modulus of concrete; I is the moment of inertia of the member's cross-section; L is the length of the structural member.

$$0.2I_g \le I_e = (0.45 + 2.5P/(A_g f_c'))/(1 + 110(d_b/h)(h/a))I_g \le I_g \tag{2}$$

$$\begin{aligned} &EI_c/EI_g = 0.2 \text{ for } P/A_g f_c' \le 0.2 \\ &(EI_c)/(EI_g) = 5P/(3A_g f_c') - 4/30 \qquad \text{for } 0.2 < P/(A_g f_c') \le 0.5 \\ &(EI_c)/(EI_g) = 0.7 \text{ when } P/(A_g f_c') > 0.5 \end{aligned} \tag{3}$$

Table 1. Effective moment of inertia according to Paulay & Priestley [9]

Structural Member	Values	Recommended value
Beam		
Rectangular section	$(0,3 \div 0,5)I_g$	$0,4I_g$
T, L section	$(0,25 \div 0,45)I_g$	$0,35I_g$
Column		
Axial load ratio >0.5	$(0,7 \div 0,9)I_g$	$0,8I_g$
Axial load ratio = 0.5	$(0,5 \div 0,7)I_g$	$0,6I_g$
Axial load ratio <0.5	$(0,3 \div 0,5)I_g$	$0,4I_g$

Elwood & Eberhard [10] investigated the influence of axial load ratio, longitudinal reinforcement diameter, shear span, and concrete compressive strength on the effective stiffness and proposed Equations 2 and 3. Similarly, according to ASCE 41-22 [7] or ACI 318-25 [8], the effective stiffness of beams, columns, and walls is recommended as presented in Table 2. While ACI 318-25 [8] permits the effective stiffness (EI_e) to be taken as $0.7EI_g$ (where EI_g denotes the stiffness of the gross, uncracked section) for columns under seismic consideration, it also provides an alternative formulation (Equation 4) to account for the effects of cracking and axial loading. Furthermore, Ngoc Tran and Li [11] proposed Equation 5 to determine EI_e based on statistical analysis of experimental data.

$$0.35EI_g \le EI_e = \left(0.8 + 25A_s/A_g\right)(1 - M_u/(P_u h))EI_g \le 0.875EI_g \tag{4}$$

$$EI_e = (2.043R_n^2 + 2.961R_n + 1.739)(3.023R_a + 2.573)EI_g \tag{5}$$

Table 2. Effective moment of inertia according to ACI 318-25 [8]

Structural member	Value
Beam	$0{,}35I_g$
Column	$0{,}7I_g$
Uncracked wall	$0{,}7I_g$
Cracked wall	$0{,}35I_g$

In Equations from 2 to 5: I_g, I_e represent the moment of inertia of the gross section and the effective moment of inertia, respectively; E, f_c' denote the modulus of elasticity and the compressive strength of the concrete prism specimen in accordance with ACI 318-25 [8]; d_b is the diameter of the longitudinal reinforcement; P is the axial compressive force; a is the shear span; h is the beam height; M_u, P_u are the ultimate moment and axial force, respectively; R_a, R_n represent the shear span ratio and axial load ratio.

Additionally, according to TCVN 9386:2012 [6], the stiffness of columns and beams is determined by Equation 6, where E and E_{cm} represent the elastic modulus of steel and concrete, respectively; r is a reduction factor dependent on the cross-sectional shape of the steel in the column, typically taken as 0.5; I_a, I_c, and I_s denote the moments of inertia of the steel section, the concrete section, and the reinforcement, respectively. For beams, two distinct flexural stiffnesses should be considered: EI_1 for the span region under positive moment (uncracked section), and EI_2 for the span region under negative moment (cracked section). Alternatively, the analysis may be conducted using an equivalent moment of inertia I_{eq} applied uniformly along the beam span, which is determined according to Equation 7. As stipulated in TCVN 9386:2012 [6], unless a more precise analysis is conducted for cracked members, the shear and elastic flexural stiffness of concrete and masonry elements may be taken as one-half of the corresponding stiffness of uncracked members.

$$(EI)_c = 0{,}9(EI_a + rE_{cm}I_c + EI_s) \tag{6}$$

$$I_{eq} = 0.6\, I_1 + 0.4\, I_2 \tag{7}$$

3. Research Results and Discussions

3.1. Evaluation of Stiffness Models for Columns

To investigate the appropriate applicability of stiffness models proposed in design codes and by various researchers, the authors utilized data from ten tested RC columns previously studied by Pham et al. [12] and Hung et al. [26]. The effective stiffness values were calculated in accordance with TCVN 9386:2012 [6], ACI 318-25 [8], Paulay & Priestley [9], Tran & Li [11], and Elwood & Eberhard [10]. The results are presented in Tables 2 and 3. Based on the analysis, the following observations can be made:

- Group 1 (high axial load ratio): this group includes specimens C-F-H, C-FS-H, and C-S-H. All models predicted higher stiffness than observed in the experimental results. Among them, the Tran & Li model yielded the closest approximation (ratio of 1.05), indicating good agreement. TCVN 9386:2012 also provided relatively accurate estimates (ratio of 1.37), suggesting its suitability for preliminary design. Conversely, ACI 318-25, Paulay & Priestley, and Elwood & Eberhard produced significantly higher estimates, indicating conservative overestimation of stiffness.
- Group 2 (low axial load ratio): this group comprises specimens C-F-L, C-FS-L, and C-S-L. In this case, TCVN 9386:2012 markedly overestimated stiffness (ratio of 2.34), rendering it unsuitable for low axial load scenarios. The Tran & Li model remained accurate (ratio of 0.94), while Elwood & Eberhard also demonstrated high stability (ratio of 1.05). ACI 318-25 and Paulay & Priestley yielded acceptable but less precise results.
- Coefficient of variation (COV): the Tran & Li model exhibited the highest stability, reflected by the lowest COV. In contrast, other methods, particularly TCVN 9386:2012 and ACI 318-25, showed greater variability.

Based on the findings, appropriate stiffness models can be selected according to the intended analytical purpose. For elements under significant axial loads or for preliminary estimations, TCVN 9386:2012 or the Tran & Li model are recommended. For low axial load conditions or nonlinear analysis requirements, the models proposed by Tran & Li or Elwood & Eberhard are preferred for their higher predictive accuracy. Moreover, in safety-oriented or conservative design contexts, models from ACI 318-25 or Paulay & Priestley should be prioritized to ensure greater safety margins.

3.2. Application of Optimal Stiffness Models to RC Frames

A seismic response simulation was conducted for RC frames using three models with varying numbers of stories: a 3-bay, 3-story frame (3B-3S), a 3-bay, 10-story frame (3B-10S), and a 3-bay, 20-story frame (3B-20S), implemented via SAP2000-v26 software [21]. Figure 1-a illustrates the typical configurations of the 10-story frame, with the latter two (3- and 20- story frames) adopting the same cross-sectional and material properties as the 10-story frame. This study aimed to investigate the stiffness degradation of RC beams and columns under seismic loading and to evaluate the resulting impacts on key structural response parameters, including roof displacement (Δ), column base moment (M), and column base shear (Q). The frame models were designed with the following specific characteristics:

- Materials: the frames were modeled using concrete with a compressive strength grade of B40, characterized by $R_b = 22\ MPa$, $R_{bt} = 1.4\ MPa$, and modulus of elasticity $E_b = 36{,}000\ MPa$. Longitudinal and transverse reinforcements in beams and columns utilized CB400V steel, with $R_s = R_sc = 350MPa$ and $E_s = 200{,}000\ MPa$.
- Geometry: to ensure uniform stiffness between beams and columns, facilitating consistent assessment of stiffness degradation, a 3-bay frame was adopted with each bay measuring $L = 3.6\ m$, and story heights of $h_t = 3.6\ m$. The total number of stories considered were 3, 10, and 20. The cross-sectional dimensions of both beams and columns were $(300 \times 600)\ mm$. Longitudinal and transverse reinforcement details for beams and columns were 8ϕ25 and ϕ8@100, respectively.
- Loading: dead and live loads were taken as 120 kN/m. Seismic loading was applied according to TCVN 9386:2012 [6], with a peak ground acceleration of $a_g = 0.4g$ for soil type B.
- Analysis model: a nonlinear analysis was conducted, incorporating plastic hinge formation in both columns and beams to capture the inelastic behavior under seismic excitation. The analysis flowchart is presented in Figure 1-b.

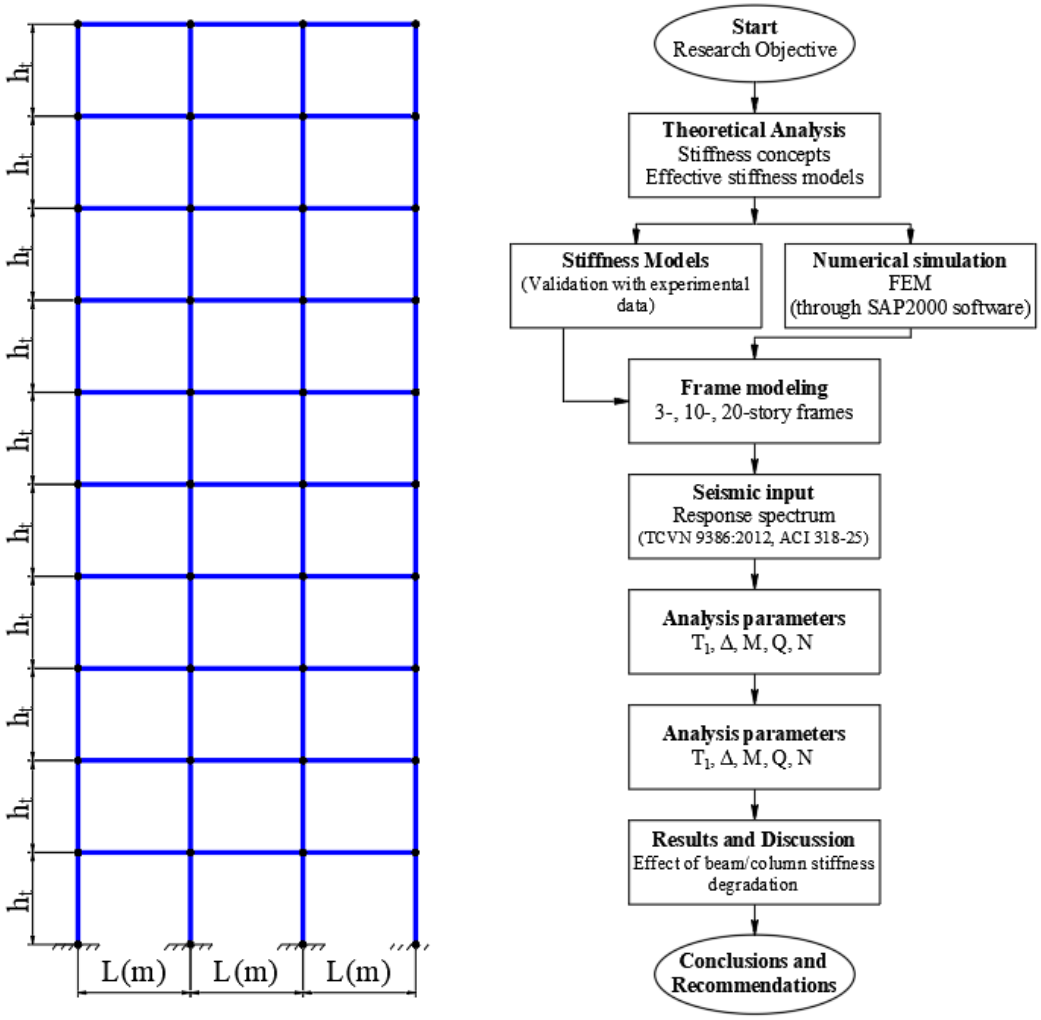

(a) RC frame model **(b) Flowchart for analysis**

Figure 1. RC frame model and analysis flowchart

3.2.1. Influence of Beam and Column Stiffness on Roof Displacement (Δ)

Figure 2 illustrates the relationship between stiffness degradation, expressed as the ratio EI_d/EI_g and the normalized roof displacement Δ/H, where H denotes the total frame height. The value Δ/H serves as an indicator of overall frame deformation under lateral loading. Each frame configuration was analyzed under three independent degradation scenarios: (i) beam stiffness reduction, (ii) column stiffness reduction, and (iii) simultaneous reduction in both beam and column stiffness. The degradation ratio EI_d/EI_g was varied from 0.1 to 1.0.

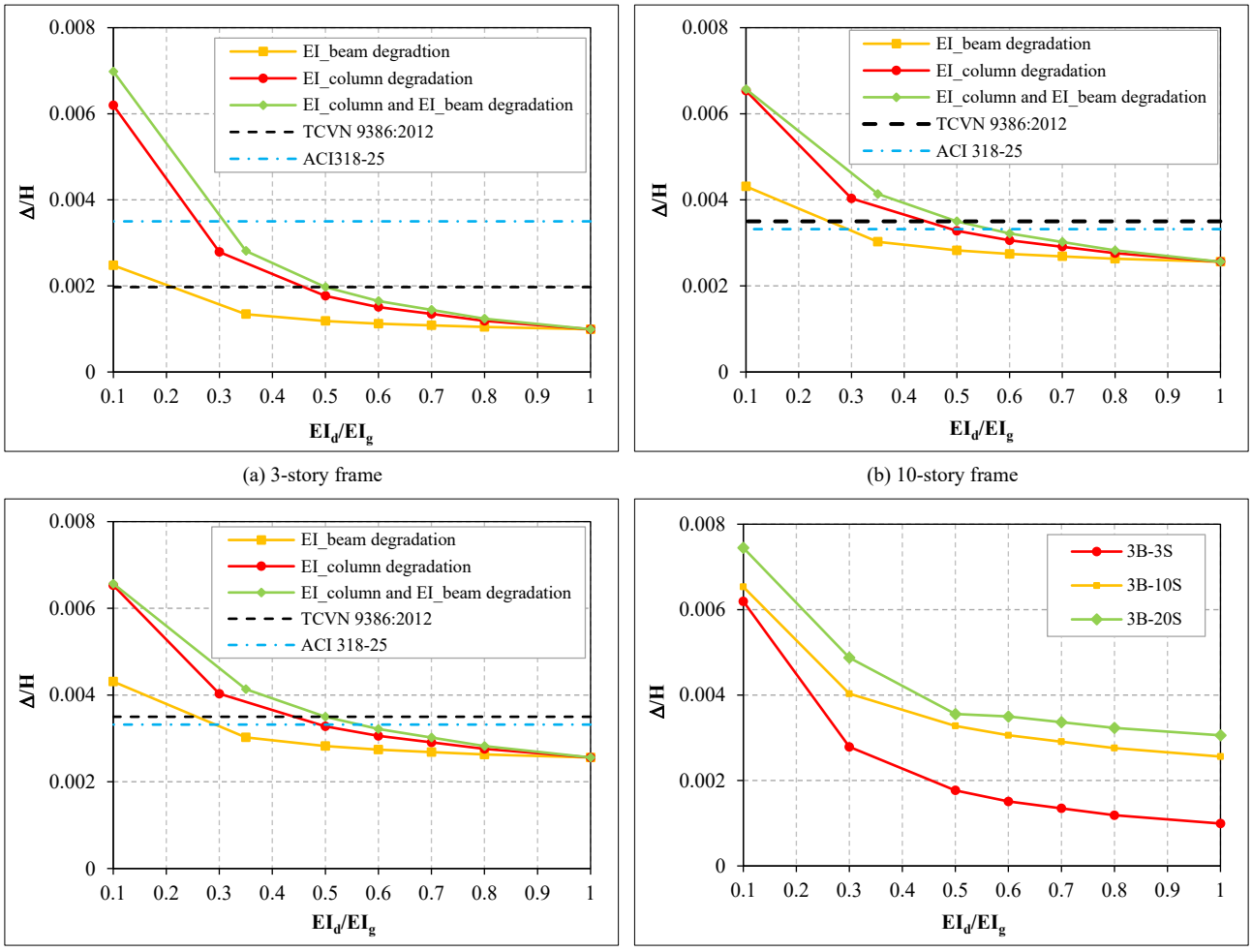

(a) 3-story frame

(b) 10-story frame

(c) 20-story frame

(d) Stiffness degradation of column section

Figure 2. Influence of stiffness degradation on roof lateral displacement (Δ)

- Figure 2-a presents the relationship between Δ/H and EI_d/EI_g for the 3-story frame. The results show a clear nonlinear reduction in Δ/H as stiffness increases, indicating that lateral deformation in low-rise frames is highly sensitive to stiffness loss, particularly in the severe degradation range $EI_d/EI_g < 0.5$. Among the three degradation scenarios, the simultaneous beam-and-column case produces the largest drift, followed by column degradation alone, while beam degradation yields the smallest displacement response. This trend confirms that even in low-rise frames, column stiffness plays a decisive role in maintaining global stability. Under extreme degradation ($EI_d/EI_g \leq 0.3$), the drift values exceed the allowable limit prescribed by TCVN 9386:2012 and approach the threshold defined by ACI 318-25, highlighting that code-based stiffness factors may underestimate actual displacements when both beams and columns deteriorate simultaneously.
- Figure 2-b shows the variation of Δ/H for the 10-story frame, where the influence of column stiffness becomes increasingly dominant. The results show that lateral deformation decreases progressively with increasing effective stiffness, revealing the nonlinear recovery of global rigidity as structural members regain stiffness. Among the three cases, the combined degradation scenario consistently produces the largest drift response, followed by the column-degradation case, while beam degradation alone exhibits the smallest displacement demand. This hierarchy indicates that column stiffness governs the overall deformation capacity of the frame and primarily controls seismic drift performance. Comparative assessment with code-based drift limits highlights notable discrepancies. For severe stiffness loss ($EI_d/EI_g < 0.5$), the simulated drift values exceed the maximum allowable limit of TCVN 9386:2012, and approach or surpass the ACI 318-25. Such exceedance suggests that the simplified stiffness reduction factors prescribed in current design standards may underestimate actual drift

when simultaneous degradation of beams and columns occurs. Conversely, as stiffness is gradually restored ($EI_d/EI_g > 0.7$), the three response curves converge, indicating that the structure reverts to a stiffness-dominant regime where deformation is less sensitive to beam flexibility.

- Figure 2-c illustrates the results for the 20-story frame, demonstrating a pronounced dependence of roof drift on column stiffness. Δ/H shows a pronounced reduction as EI_d/EI_g increases, confirming that stiffness recovery substantially mitigates lateral deformation. At the extreme degradation stage ($EI_d/EI_g \leq 0.3$), drift responses differ markedly among scenarios, indicating that the contribution of each structural component to global stiffness is highly nonuniform. The combined degradation case consistently produces the highest deformation, while column degradation alone results in slightly lower but still critical drift values. In contrast, beam degradation leads to the most stable and limited displacement response throughout the entire stiffness range, emphasizing its secondary role in drift control compared with column stiffness. When benchmarked against code provisions, the results demonstrate that under severe degradation ($EI_d/EI_g < 0.5$), both the combined and column-degradation cases exceed the TCVN 9386:2012, and approach or surpass the ACI 318-25, particularly within the high nonlinearity range. These exceedances reveal that current empirical stiffness reduction factors in both codes may underestimate displacement demand in nonlinear conditions where degradation occurs simultaneously in beams and columns. As stiffness approaches the elastic state ($EI_d/EI_g > 0.7$), all three curves gradually converge, suggesting that beyond partial recovery, additional stiffness restoration yields diminishing returns in drift reduction.
- Figure 2-d synthesizes the variation of Δ/H with respect to EI_d/EI_g for the three representative RC frame configurations (3B-3S, 3B-10S, and 3B-20S). The general trend reveals a nonlinear reduction of Δ/H as the effective stiffness increases, confirming that the recovery of member stiffness directly enhances global lateral rigidity. Nevertheless, the magnitude and rate of drift reduction are strongly dependent on building height, demonstrating the height-sensitive nature of stiffness degradation in reinforced concrete frames. For the low-rise frame, Δ/H decreases sharply as EI_d/EI_g increases from 0.1 to 0.5, after which the curve stabilizes near a minimal. This rapid decline indicates that the structural stiffness of low-rise frames is highly responsive to even small improvements in member stiffness, primarily because beam stiffness dominates the lateral resistance mechanism. In contrast, the 10-story and 20-story frames exhibit much flatter slopes, even when EI_d/EI_g approaches unity. These results highlight that taller frames retain higher lateral flexibility due to the increasing dominance of column deformation and $P-\Delta$ effects. A cross-comparison among the three models reveals that, at extreme degradation levels ($EI_d/EI_g \leq 0.3$), the 20-story frame experiences a roof drift nearly four times that of the 3-story model. When benchmarked against code-based limits, the drift of the 3-story frame remains below the TCVN 9386:2012 across all degradation ratios, while the 10-story frame slightly exceeds this limit under $EI_d/EI_g < 0.5$. The 20-story frame shows the most critical response, with Δ/H consistently surpassing the allowable drifts of both TCVN 9386:2012 and ACI 318-25 even under moderate stiffness reduction. These findings clearly demonstrate that conventional stiffness reduction factors in seismic codes may be adequate for low-rise buildings but can underestimate displacement demand for medium- and high-rise structures.

On the whole, the results presented in Figure 2 reveal a distinct nonlinear relationship between Δ/H and EI_d/EI_g, with the response strongly governed by both the degradation level and the building height. the results collectively reveal that Δ is governed by a complex interaction between stiffness degradation and structural height. In the low-rise frame, reductions in beam stiffness have the most pronounced impact on Δ, demonstrating that horizontal members primarily control lateral deformation in short, squat systems. This observation aligns with the findings of Paulay & Priestley [9], who emphasized the contribution of beam flexural stiffness to global stability in low-rise RC frames. In the extreme degradation range ($EI_d/EI_g < 0.3$), all frames exhibit substantial increases in lateral drift, confirming that global deformation is highly sensitive to stiffness loss at this stage. The simultaneous beam-and-column degradation consistently produces the largest displacements, followed by column degradation alone, while beam degradation has only a minor effect. Under these conditions, the 10- and 20-story frames exceed the allowable drift limits specified in TCVN 9386:2012 and approach or surpass the ACI 318-25 thresholds, highlighting the pronounced vulnerability of tall RC frames to column softening. In the moderate degradation range ($0.3 \leq EI_d/EI_g \leq 0.5$), the rate of drift reduction becomes more gradual, marking a transition between nonlinear softening and partial stiffness recovery. The low-rise frame shows a sharp decline in Δ/H, reflecting its high responsiveness to even small stiffness improvements due to beam-dominated lateral resistance. In contrast, the mid- and high-rise frames still exhibit large residual deformations within this range, indicating that column stiffness remains the controlling factor in restoring lateral rigidity. As the stiffness ratio increases further into the partial recovery range ($0.5 < EI_d/EI_g \leq 0.7$), the drift curves of all scenarios begin to converge, suggesting that the structural system gradually shifts toward a stiffness-dominant regime. Although deformations continue to decrease, the rate of improvement diminishes, implying that additional stiffness restoration yields limited benefits in drift reduction. This stage represents the onset of dynamic stabilization, where column integrity governs the overall response and beam flexibility becomes negligible. Finally, in the elastic or near-recovered state ($EI_d/EI_g > 0.7$), Δ/H approaches a steady value, and the differences between beam, column, and combined degradation scenarios become insignificant. The structural response in this range indicates that sufficient stiffness recovery effectively mitigates nonlinear deformation, restoring the global rigidity of the frame. Moreover, the findings confirm

that the influence of stiffness degradation on roof drift is highly height-dependent and nonlinear. Beam stiffness primarily controls deformation in low-rise frames, whereas column stiffness dictates the lateral response of medium- and high-rise systems. The analysis also demonstrates that existing code-based stiffness reduction factors are generally adequate for short structures but tend to underestimate displacement demands in taller frames, particularly when degradation extends below $EI_d/EI_g = 0.5$. Accurate modeling of both beam and column stiffness degradation, especially in the severe and moderate ranges, is therefore essential for achieving reliable predictions of seismic drift and for ensuring compliance with displacement control requirements prescribed in TCVN 9386:2012 and ACI 318-25.

3.2.2. Influence of Beam and Column Stiffness on the Fundamental Period (T_1)

Figure 3 presents the relationship between the stiffness degradation ratio (EI_d/EI_g) and the fundamental period (T_1) of the RC frame. This parameter characterizes the global dynamic response of the structure and reflects its overall stiffness and flexibility under seismic excitation. Examining variations in T_1 under different stiffness degradation scenarios clarify the relative contribution of beam and column stiffness and highlights the influence of building height on the dynamic characteristics of RC frames.

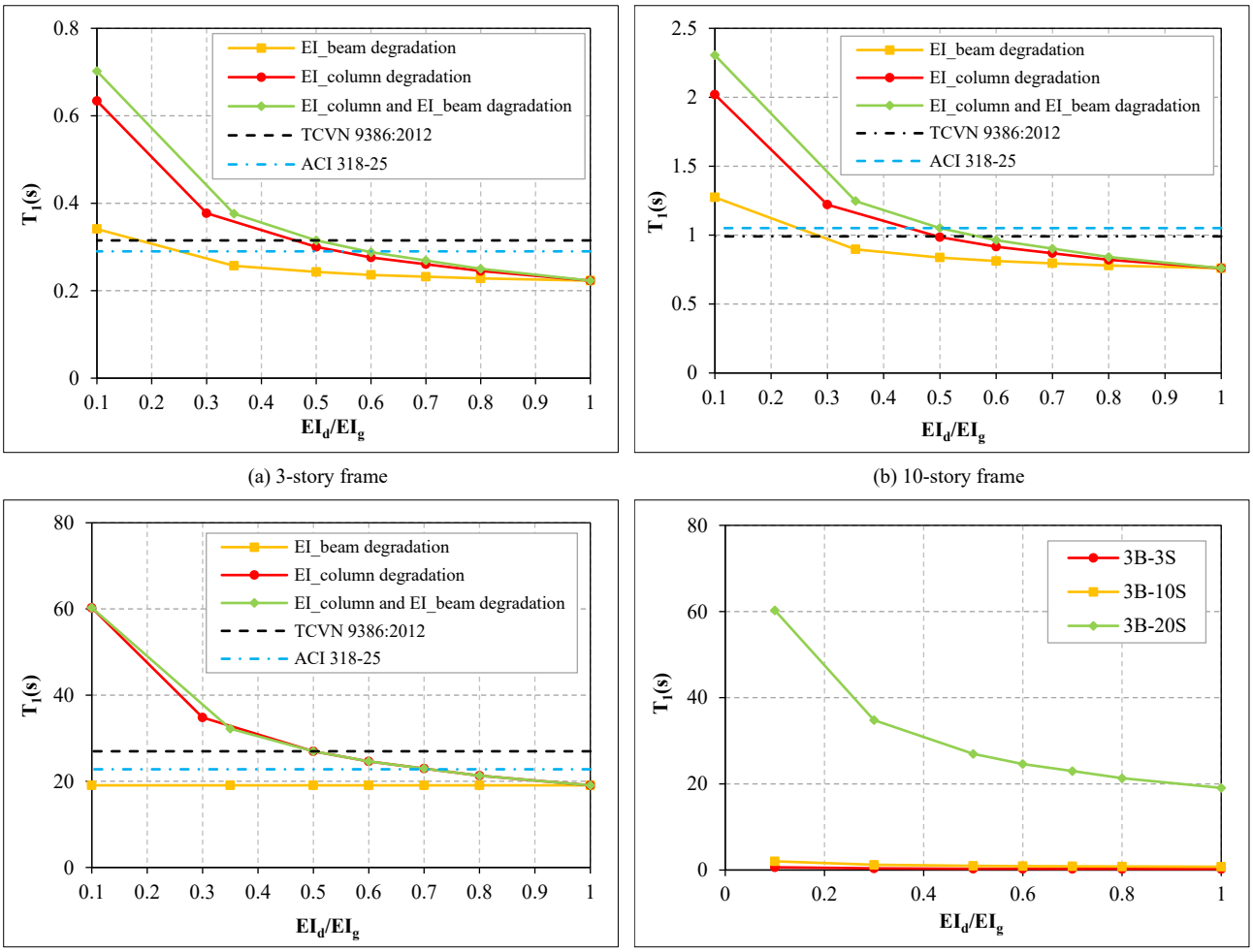

(a) 3-story frame

(b) 10-story frame

(c) 20-story frame

(d) Stiffness degradation of column section

Figure 3. Influence of stiffness degradation on the fundamental period (T_1)

- The results presented in Figure 3-a demonstrate that T_1 is highly sensitive to the degree and location of stiffness degradation. A clear nonlinear trend is observed, where T_1 decreases progressively as the effective stiffness ratio EI_d/EI_g increases, indicating a gradual restoration of global rigidity. In the beam-degradation scenario, the period variation is relatively minor, suggesting that beam stiffness has a limited contribution to the global dynamic response. By contrast, the reduction of column stiffness leads to a significant elongation of T_1, particularly at severe degradation levels ($EI_d/EI_g < 0.5$), emphasizing the dominant role of columns in governing the overall vibration characteristics of RC frames. The combined degradation of both beams and columns yields the longest periods across all stiffness levels, confirming the cumulative influence of multi-member stiffness loss on global flexibility. When compared with the code-based reference values, the computed periods for the column-only and combined degradation cases exceed the upper bounds recommended by TCVN 9386:2012 and ACI 318-25, especially under pronounced stiffness deterioration. Such exceedance indicates that the simplified stiffness-reduction factors specified in design standards

may underestimate the actual dynamic response of degraded structures. As stiffness is gradually restored ($EI_d/EI_g > 0.7$), all three curves converge toward similar values, suggesting that the structural period becomes less sensitive to beam stiffness once the elastic regime is approached.

- The results in Figure 3-b reveal a strong dependence of T_1 on both the degree and location of stiffness degradation. In general, T_1 increases markedly as the effective stiffness ratio EI_d/EI_g decreases, indicating that global flexibility grows rapidly when member stiffness deteriorates. Among the three scenarios, the combined beam-and-column degradation produces the largest period elongation, followed by column-only degradation, while beam degradation alone results in the smallest increase. This behavior highlights the governing role of column stiffness in controlling the dynamic response of high-rise RC frames. When column stiffness is reduced to $EI_d/EI_g < 0.3$, T_1 nearly doubles compared with the undegraded condition, reflecting a substantial loss of lateral rigidity and an increased susceptibility to resonance. When benchmarked against design standards, the computed periods under column and combined degradation exceed the upper bounds prescribed by TCVN 9386:2012 and ACI 318-25, particularly in the severe degradation range. These exceedances imply that the empirical stiffness reduction factors recommended in current codes may not adequately represent the dynamic behavior of deteriorated high-rise frames. In contrast, the beam degradation scenario remains within the allowable period range, reaffirming that beam stiffness has a secondary influence on global vibration characteristics. As EI_d/EI_g approaches unity, all three response curves converge toward approximately $T_1 = 0.76$ s, indicating that period elongation stabilizes once stiffness recovery occurs. On the whole, the results demonstrate that column stiffness degradation dominates the evolution of T_1 in tall frames, while beam deterioration contributes only marginally. The elongation of the fundamental period under column softening amplifies seismic demand by shifting the structure toward longer-period regions of the response spectrum. Therefore, for high-rise systems, accurate representation of column stiffness reduction is essential to ensure realistic estimation of dynamic characteristics and to maintain consistency with the vibration limits required by TCVN 9386:2012 and ACI 318-25.
- The results in Figure 3-c demonstrate that T_1 of the 20-story RC frame is extremely sensitive to stiffness degradation, particularly at low EI_d/EI_g ratios. A pronounced nonlinear increase in T_1 is observed as stiffness decreases, indicating that high-rise structures experience substantial flexibility loss even under moderate degradation. Among the three scenarios, the combined beam-and-column degradation yields the longest period, followed closely by column degradation alone, while beam degradation produces the least variation. This hierarchy confirms that in tall buildings, column stiffness predominantly controls the dynamic response, whereas beam stiffness contributes marginally to overall system rigidity. At severe degradation levels ($EI_d/EI_g < 0.3$), the period of the combined-degradation case increases to more than three times that of the undegraded model, reaching approximately 60 s. Such elongation far exceeds the upper limits recommended by TCVN 9386:2012 and ACI 318-25, underscoring the inadequacy of existing empirical stiffness-reduction factors for tall RC frames. In contrast, the beam-only degradation scenario maintains a nearly constant period around 20 s, suggesting that horizontal member deterioration alone does not significantly affect the fundamental mode. As stiffness gradually recovers ($EI_d/EI_g > 0.7$), all three curves converge, indicating that the influence of degradation diminishes once the elastic stiffness is regained.
- Figure 3-d summarizes the relationship between T_1 and EI_d/EI_g for the three representative RC frame configurations (3B-3S, 3B-10S, and 3B-20S). The overall trend reveals that T_1 decreases progressively as stiffness is restored, reflecting the gradual recovery of structural rigidity. However, the magnitude and sensitivity of period variation differ significantly with building height, demonstrating the height-dependent influence of stiffness degradation on the dynamic behavior of RC frames. In the 3B-3S frame, the period remains nearly constant across all stiffness ratios, indicating that stiffness degradation has only a minor effect on the dynamic response of low-rise structures, where beam stiffness and low slenderness ratios dominate system rigidity. For the 10-story frame, a slight increase in T_1 is observed at severe degradation levels ($EI_d/EI_g < 0.3$), but the variation remains limited, suggesting moderate sensitivity to column stiffness reduction. In contrast, the 20-story model exhibits a pronounced nonlinear response: as stiffness decreases, T_1 rises sharply, from about 20 s in the undegraded condition to over 60 s when $EI_d/EI_g = 0.1$, indicating substantial flexibility and strong dependence on column integrity.

In summary, the results in Figure 3 demonstrate a distinct nonlinear relationship between T_1 and EI_d/EI_g, exhibiting clear height-dependent characteristics across the three analyzed RC frame configurations. The remarkable period elongation observed in the high-rise frame aligns with the findings of Di Sarno & Amiri [27], who reported similar amplification effects in deteriorated tall structures. In the severe degradation range ($EI_d/EI_g < 0.3$), T_1 increases sharply for all models, indicating a substantial loss of global rigidity and a rapid transition of the system into a highly flexible state. The elongation of T_1 is most pronounced in the column and combined degradation cases, confirming that column stiffness is the primary factor governing the dynamic response. Under these conditions, the computed periods exceed the upper limits prescribed by TCVN 9386:2012 and ACI 318-25, particularly for the 10- and 20-story frames, signifying that tall RC buildings are highly susceptible to column softening and corresponding period elongation. In the moderate degradation range ($0.3 \leq EI_d/EI_g \leq 0.5$), the period continues to lengthen but at a reduced rate, marking the onset of partial stiffness recovery. The 3-story frame exhibits only a minor change in T_1, whereas the 10- and 20-story frames show sustained elongation due to the progressive recovery of column stiffness and redistribution of internal forces. This

range reflects the transitional phase where dynamic sensitivity to stiffness degradation remains high, and small variations in stiffness can significantly alter the global vibration characteristics. As the structure enters the partial recovery range ($0.5 < EI_d/EI_g \leq 0.7$), the rate of period reduction becomes moderate and the differences among the three degradation scenarios narrow. The system progressively regains rigidity, and the influence of beam degradation becomes negligible compared with column stiffness restoration. For tall frames, however, T_1 remains considerably higher than the undegraded state, suggesting that even partial stiffness recovery does not fully restore the original dynamic properties. In the near-elastic regime ($EI_d/EI_g > 0.7$), the period curves for all scenarios converge, signifying that the frame behaves predominantly in the elastic range and that further stiffness restoration yields diminishing changes in dynamic response. At this stage, T_1 stabilizes, and the lateral stiffness of columns governs the overall vibration behavior of the entire system. Collectively, these results confirm that the elongation of the fundamental period is highly nonlinear and height-dependent. Beam stiffness reduction has a limited effect on T_1 in low-rise structures, while column stiffness degradation overwhelmingly controls dynamic flexibility in medium- and high-rise frames. When $EI_d/EI_g < 0.5$, the period elongation becomes critical, potentially amplifying seismic demand by shifting the structure into the long-period region of the response spectrum. Therefore, accurate representation of column stiffness degradation across the full stiffness-reduction range is essential for realistic prediction of dynamic characteristics and for ensuring compliance with the vibration limits stipulated by TCVN 9386:2012 and ACI 318-25 in the seismic design of RC frame structures.

3.2.3. Influence of Beam and Column Stiffness on Column Base Moment (M)

Figure 4 illustrates the relationship between the stiffness degradation ratio (EI_d/EI_g) and the maximum moment at the column base (M). This parameter reflects the degree of internal force concentration at the foundation, an area most affected by lateral system responses. Examining variations in M under different stiffness degradation scenarios clarify the role of individual structural elements (beam or column) and the influence of building geometry on internal force distribution under nonlinear conditions.

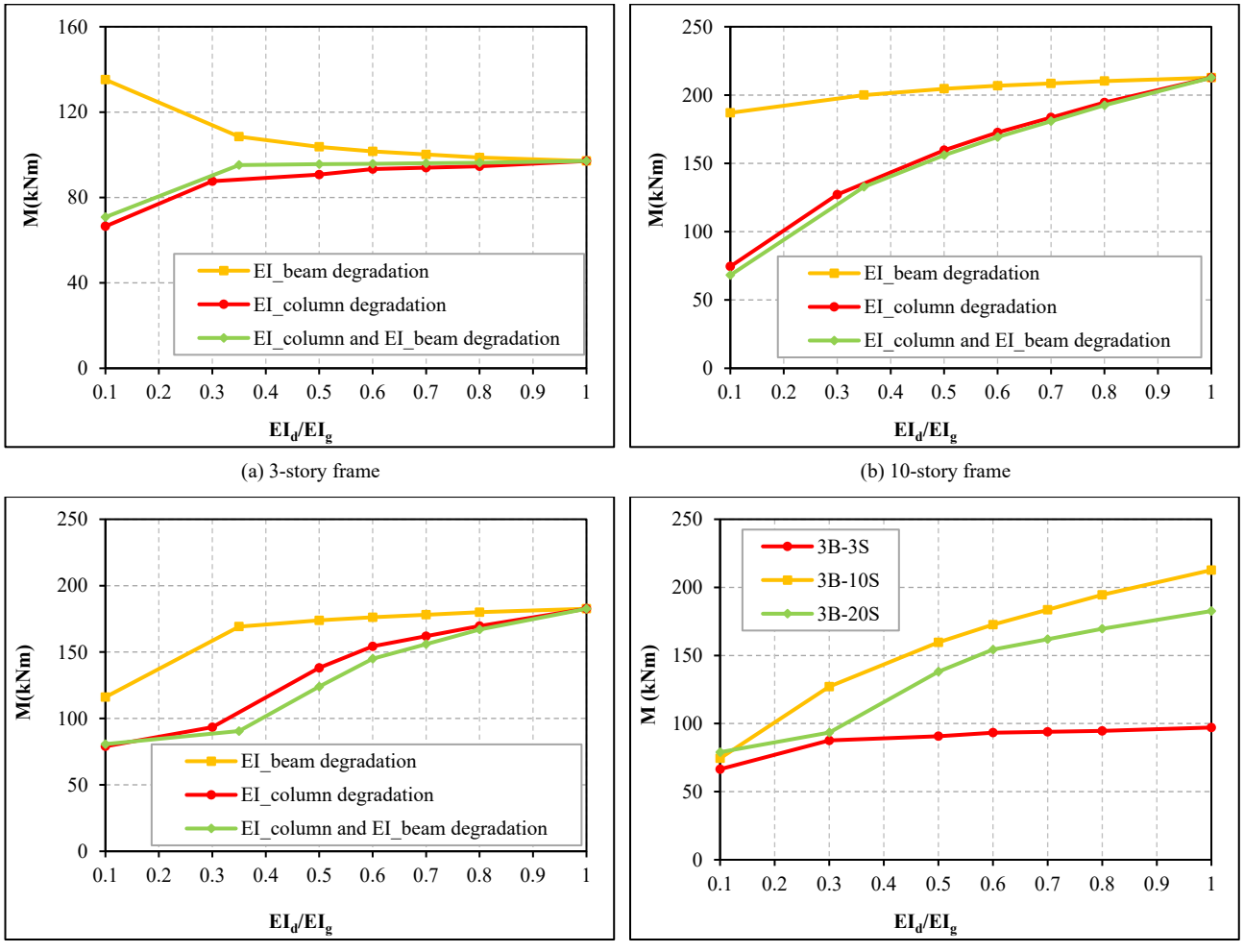

(a) 3-story frame

(b) 10-story frame

(c) 20-story frame

(d) Stiffness degradation of column section

Figure 4. Influence of stiffness degradation on column base moment (M)

- Figure 4-a shows the relationship between M and stiffness degradation for the 3-story frame. The results indicate that beam stiffness degradation leads to a clear reduction in M, particularly when $EI_d/EI_g < 0.3$, as the increased beam

flexibility releases moment transfer at the column base. Conversely, column degradation produces a gradual increase in M as stiffness recovers, suggesting enhanced force concentration in the lower stories once column rigidity is regained. The combined degradation scenario exhibits an intermediate response, with M stabilizing at approximately 90 kNm for $EI_d/EI_g > 0.5$. These results imply that in low-rise structures, beam flexibility plays a greater role in reducing base moment demand, while columns remain the primary contributors to overall force transfer during stiffness recovery.

- Figure 4-b presents the variation of M for the 10-story frame, where the influence of column stiffness becomes more dominant. Under severe degradation ($EI_d/EI_g < 0.3$), all cases show relatively low moment demands due to overall structural softening. However, as stiffness is restored, M increases markedly, especially in the beam degradation scenario, which reaches the highest base moments due to the inability of flexible beams to share lateral loads effectively. In contrast, column degradation produces smaller M values at the same stiffness levels, indicating that the weakened columns redistribute internal forces upward rather than concentrating them at the base. The combined degradation case follows a nearly linear increase, reflecting a balanced interaction between beam and column stiffness recovery.
- Figure 4-c illustrates the results for the 20-story frame, where the effect of column stiffness degradation is most pronounced. At low stiffness ratios ($EI_d/EI_g < 0.3$), all models display limited moment transfer to the foundation because of the high overall flexibility of the tall structure. As stiffness increases, M rises significantly, particularly for the beam degradation case, which exhibits the highest base moments once rigidity is regained. This suggests that in tall frames, beam softening reduces the redistribution capacity of the lateral system, forcing greater moment concentration into the column bases. The column degradation scenario, however, produces lower M values at early degradation stages and converges to the other cases at higher stiffness ratios, confirming that column stiffness governs the ultimate internal force distribution in high-rise systems.
- Figure 4-d provides a comparative summary of base moment variation among the three frame heights. The results clearly demonstrate a height-dependent trend: as building height increases, the base moment magnitude grows significantly for the same stiffness ratio, reflecting the increased overturning demand and the larger lever arm of lateral forces in tall structures. The 3-story frame maintains the smallest and most stable M values, while the 10- and 20-story frames show progressively higher and more sensitive responses to stiffness degradation. Under partial stiffness recovery ($EI_d/EI_g > 0.7$), all frames converge toward similar M values, indicating that structural stiffness restoration mitigates height effects. Overall, these findings confirm that column stiffness degradation plays a decisive role in base moment amplification in medium- and high-rise RC frames, emphasizing the necessity of incorporating accurate stiffness degradation models in nonlinear seismic analysis.

In general, the findings illustrated in Figure 4 indicate that M varies nonlinearly with stiffness degradation and exhibits a clear dependence on both degradation level and building height. In the severe degradation range ($EI_d/EI_g < 0.3$), M remains relatively low for all cases due to the overall loss of stiffness and lateral resistance. In low-rise frames, beam degradation reduces moment transfer to the column base because increased beam flexibility alleviates joint restraint and dissipates internal forces away from the foundation. In contrast, column degradation and combined degradation produce slightly higher M values as the loss of column rigidity limits lateral load redistribution, especially in medium- and high-rise frames. In the moderate degradation range ($0.3 \leq EI_d/EI_g \leq 0.5$), base moments start to increase as stiffness recovery begins. The 10- and 20-story frames show a more rapid rise in M compared to the 3-story model, indicating that column stiffness restoration strongly influences force concentration at the base in taller structures. The beam degradation scenario yields the steepest increase in M during this phase, reflecting the inability of flexible beams to share loads efficiently, which forces larger bending demands into the columns. This trend highlights the shift from a beam-dominated mechanism in short frames to a column-dominated one in tall systems.

As stiffness continues to recover in the partial recovery range ($0.5 < EI_d/EI_g \leq 0.7$), the rate of moment amplification slows, and the differences among the three degradation scenarios begin to diminish. M approaches stable values in low-rise frames, while mid- and high-rise models still experience moderate increases, suggesting that partial recovery of column stiffness reinstates force concentration at the base but also enhances overall system stability. In the near-elastic regime ($EI_d/EI_g > 0.7$), the moment curves for all frames converge toward similar values, implying that stiffness restoration effectively mitigates height-dependent differences in internal force distribution. Nonetheless, tall frames consistently exhibit higher M values than short ones, reflecting greater overturning moments associated with their increased height-to-span ratios. Overall, the results confirm that column stiffness degradation is the primary driver of base moment amplification in medium- and high-rise frames, while beam degradation mainly influences low-rise systems by temporarily reducing moment transfer. Misrepresentation of stiffness degradation can therefore lead to either underestimation or overestimation of base moments, depending on the structural height. Accurate modeling of both beam and column stiffness degradation, particularly within the $EI_d/EI_g < 0.5$ range, is essential to ensure reliable evaluation of internal force demands and to enhance the predictive capability of nonlinear seismic analysis in reinforced concrete frame structures.

3.2.4. Influence of Beam and Column Stiffness on Column Base Shear (Q)

Figure 5 illustrates the relationship between the stiffness degradation ratio (EI_d/EI_g) and the maximum shear force at the column base (Q). This parameter represents the total lateral force transferred to the foundation and is a key design criterion for assessing the strength of the foundation and shear-resisting system. Analyzing the variation of Q under different levels of flexural stiffness degradation provides insight into the frame's lateral load transmission capability.

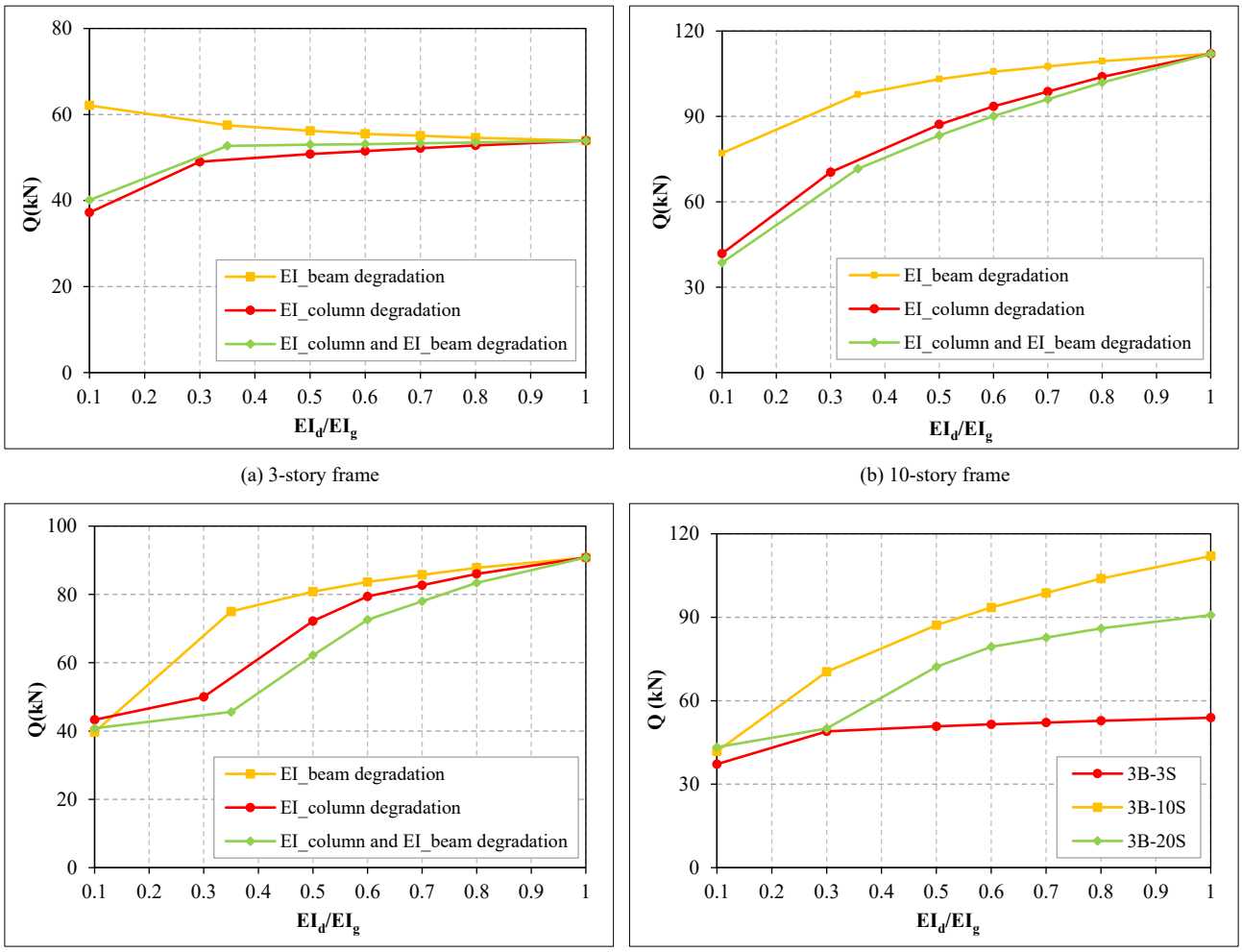

(a) 3-story frame

(b) 10-story frame

(c) 20-story frame

(d) Stiffness degradation of column section

Figure 5. Influence of stiffness degradation on column base shear (Q)

- Figure 5-a illustrates the relationship between Q and stiffness degradation for the 3-story frame. The results show that beam stiffness reduction slightly decreases Q at degradation levels $EI_d/EI_g < 0.3$, as the flexible beams reduce lateral force transfer to the column bases. In contrast, column degradation and combined degradation scenarios cause a gradual increase in Q as stiffness is restored, reaching similar values beyond $EI_d/EI_g > 0.7$. This behavior suggests that in low-rise frames, both beams and columns share the lateral load-resisting mechanism, with beam stiffness playing a more prominent role in reducing shear transfer under high flexibility conditions.
- Figure 5-b presents the variation of Q for the 10-story frame, where the influence of column stiffness degradation becomes more pronounced. At $EI_d/EI_g < 0.3$, all cases exhibit small shear forces due to system softening; however, as stiffness recovers, Q increases rapidly, particularly in the beam-degradation case. The higher Q values associated with beam degradation indicate that weakened beams lose their ability to redistribute lateral forces, concentrating greater shear demand at the column bases. The combined degradation scenario yields intermediate results, reflecting the combined effects of reduced stiffness and force redistribution within the frame.
- Figure 5-c shows the behavior of the 20-story frame, highlighting the dominant role of columns in tall structures. Under severe degradation ($EI_d/EI_g < 0.3$), Q remains relatively low for all scenarios, corresponding to a highly flexible lateral system. As stiffness increases, however, the base shear rises sharply, especially for the beam-degradation case, which exhibits the largest Q values once rigidity is restored. This indicates that beam softening in tall frames limits the redistribution capacity of the lateral system, forcing higher shear demands into the columns. Meanwhile, column degradation results in delayed shear recovery, confirming that column stiffness primarily governs base shear in high-rise systems.

- Figure 5-d provides a comparative summary of Q for the three frame heights. The results reveal a strong height-dependent trend: as building height increases, the base shear magnitude grows substantially for the same stiffness ratio. The 3-story frame displays the lowest Q values and the least sensitivity to stiffness degradation, whereas the 10- and 20-story frames show progressively larger and more responsive Q variations. This indicates that the contribution of column stiffness to shear resistance intensifies with height. Beyond $EI_d/EI_g > 0.7$, all models converge, suggesting that stiffness recovery mitigates height effects on shear distribution. Overall, these findings confirm that column stiffness degradation controls the shear behavior of tall RC frames, while beam degradation mainly affects low-rise configurations.

In summary, the results presented in Figure 5 demonstrate Q exhibits a nonlinear dependence on stiffness degradation and building height, reflecting the complex redistribution of lateral forces as member stiffness changes. In the severe degradation range ($EI_d/EI_g < 0.3$), Q remains relatively low for all models due to overall system flexibility and reduced capacity for lateral force transfer. In this stage, beam degradation slightly decreases Q in low-rise frames, as flexible beams reduce joint restraint and diminish the direct transmission of shear to the column bases. Conversely, in taller frames, even minor column degradation markedly limits lateral resistance, resulting in significantly lower shear demands and delayed force recovery. In the moderate degradation range ($0.3 \leq EI_d/EI_g \leq 0.5$), base shear begins to increase as stiffness is partially regained. The rate of growth is particularly evident in the beam-degradation scenario, where weakened beams are unable to distribute lateral forces effectively, thereby concentrating larger shear demands on the columns. This behavior is more pronounced in medium- and high-rise frames, indicating that the redistribution capacity of the system depends strongly on column stiffness restoration. The combined degradation case yields intermediate results, suggesting a balanced yet limited recovery of lateral load transfer mechanisms. As the structure transitions into the partial recovery range ($0.5 < EI_d/EI_g \leq 0.7$), Q increases steadily and the differences between the three degradation scenarios begin to diminish. In this regime, the reactivation of column stiffness enhances the frame's ability to resist lateral forces, while beam stiffness recovery contributes minimally to the overall shear response.

The 10- and 20-story models exhibit a more pronounced shear amplification than the 3-story frame, emphasizing the greater sensitivity of tall structures to stiffness variations. In the near-elastic regime ($EI_d/EI_g > 0.7$), all models converge toward similar shear capacities, indicating that sufficient stiffness recovery mitigates the effect of height and member degradation on shear distribution. However, the absolute magnitude of Q remains higher in taller frames, reflecting the increased overturning and inertial forces associated with greater structural height. Overall, the results confirm that column stiffness degradation is the dominant factor controlling base shear behavior in medium- and high-rise RC frames, while beam stiffness reduction primarily influences shear transfer in low-rise structures. The critical range $EI_d/EI_g < 0.5$ represents the most sensitive phase of nonlinear shear response, where misrepresentation of stiffness degradation can lead to unsafe underestimation of lateral force demands. Accurate modeling of stiffness loss, especially in columns, is therefore essential to ensure reliable prediction of base shear and to maintain compliance with the seismic design requirements stipulated in TCVN 9386:2012 and ACI 318-25.

The overall findings indicate that the seismic responses of RC frames vary distinctly across four stiffness degradation ranges:

- Severe degradation ($EI_d/EI_g < 0.3$): At this stage, the structural stiffness is significantly reduced, leading to critical nonlinear responses. Δ/H increases sharply, often exceeding the allowable limits of TCVN 9386:2012 and approaching ACI 318-25 thresholds, particularly in tall frames. T_1 elongates rapidly, up to two to three times its elastic value, indicating a pronounced loss of global rigidity and a shift into the long-period region of the seismic spectrum. M and Q remain relatively low because of the overall flexibility of the system; however, load redistribution becomes unstable. This phase represents the most critical condition where simultaneous beam–column degradation yields the most unfavorable performance.
- Moderate degradation ($0.3 \leq EI_d/EI_g \leq 0.5$): Partial recovery of stiffness begins, yet the structural response remains highly nonlinear. Δ/H decreases gradually but still exceeds code-based drift limits for medium- and high-rise frames. T_1 remains elongated due to incomplete stiffness restoration, while M and Q start to increase as lateral stiffness and force transfer mechanisms re-engage. Beam flexibility contributes to higher base moments in this range, especially when column stiffness is still limited. The system is most sensitive to column degradation in this interval, making it a transitional zone between instability and recovery.
- Partial recovery ($0.5 < EI_d/EI_g \leq 0.7$): The structure regains much of its lateral rigidity. Δ/H and T_1 both show marked stabilization, and the differences between degradation scenarios narrow. M and Q increase moderately with stiffness restoration, particularly in tall frames, where column stiffness dominates internal force concentration. The influence of beam degradation becomes negligible, while column stiffness governs both the amplitude and distribution of seismic demand. This range represents a semi-stable regime where stiffness recovery effectively limits further deformation.
- Near-elastic regime ($EI_d/EI_g > 0.7$): The frames behave almost elastically, with Δ/H and T_1 reaching stable values close to the undegraded condition. M and Q converge among all scenarios, indicating that additional stiffness

recovery has minimal effect on global response. Height-related differences diminish, and the structural system transitions fully into a stiffness-controlled state with stable lateral load transfer.

Overall, the findings confirm that stiffness degradation below 0.5 is the most critical range for seismic performance, where rapid deterioration in Δ/H and T_1 coincides with unstable M and Q redistribution. In contrast, partial recovery above 0.5 effectively restores global stiffness and stabilizes internal forces. Beam stiffness governs drift and force redistribution in low-rise frames, whereas column stiffness dominates the dynamic and internal force responses in medium- and high-rise systems. Existing stiffness-reduction factors in TCVN 9386:2012 and ACI 318-25 are adequate for mild degradation but tend to underestimate deformation and internal forces in the nonlinear regime ($EI_d/EI_g < 0.5$). Accurate modeling of both beam and column stiffness degradation, especially within this critical range, is essential to ensure reliable seismic evaluation and performance-based design of RC frame structures.

4. Conclusion

This study investigated the influence of stiffness degradation on the seismic performance of RC frames through nonlinear analysis using SAP2000. Four key response parameters - roof lateral displacement ratio (Δ/H), fundamental period (T_1), column base moment (M), and column base shear (Q) - were examined across three frame heights (3-, 10-, and 20-story) under three degradation scenarios: beam-only, column-only, and combined stiffness reduction. The results reveal a clear height-dependent pattern in the structural response. In the low-rise 3-story frame, beam stiffness degradation primarily governs lateral deformation, as beam flexibility directly influences roof drift and moment redistribution. In contrast, for the 10- and 20-story frames, column stiffness degradation becomes the decisive factor controlling global behavior. Even moderate column softening ($EI_d/EI_g < 0.5$) markedly increases roof displacement and elongates the fundamental period, shifting the dynamic behavior toward the critical long-period region of the response spectrum. Simultaneous degradation of beams and columns produces the most unfavorable outcomes, including excessive drifts, extended vibration periods, and unstable internal force redistribution. The analyses of M and Q further confirm that column stiffness dictates lateral load transfer in medium- and high-rise frames, while beam stiffness mainly affects low-rise configurations. Beam degradation alleviates base moment demand in short structures but amplifies internal forces in taller systems as stiffness is restored. Conversely, column degradation dominates both the magnitude and evolution of M and Q. Inaccurate modeling of column stiffness loss may therefore lead to unsafe underestimation of seismic demand and excessive flexibility in tall buildings.

These findings emphasize the need for height-sensitive stiffness degradation modeling. Beam stiffness governs local deformation and drift control in short frames, whereas column stiffness determines dynamic characteristics, internal force distribution, and overall stability in taller structures. Current effective stiffness formulations in TCVN 9386:2012 and ACI 318-25 may not fully capture nonlinear degradation effects, particularly under simultaneous member deterioration. Among the evaluated approaches, the Tran & Li formulation exhibited the highest accuracy and stability when validated against experimental data, demonstrating its suitability for advanced nonlinear seismic analysis. Practical recommendations for design can be drawn from the results. In high-rise buildings, column stiffness should not be reduced below 0.5 of the gross section stiffness ($EI_d/EI_g \geq 0.5$) to maintain acceptable vibration periods and prevent excessive lateral drift. For performance-based seismic design, stiffness degradation models should explicitly incorporate building height and member type to ensure compliance with displacement and period limits prescribed by modern design standards. The proposed stiffness thresholds and modeling recommendations can be readily implemented in seismic design and assessment workflows using commercial FEM software such as SAP2000 or ETABS, allowing engineers to achieve more accurate yet computationally efficient evaluations of RC frame behavior. The novelty of this research lies in quantifying the nonlinear, height-dependent influence of stiffness degradation across multiple structural parameters ($\Delta/H, T_1, M, Q$), thereby providing a unified framework for linking component-level stiffness deterioration with system-level seismic performance assessment of RC frames.

However, this research has several limitations. The analyses were conducted on planar frame models, which do not fully represent three-dimensional effects such as torsional response and floor diaphragm interaction. Seismic loading was applied using the response spectrum method, without incorporating nonlinear time-history analyses that may capture cyclic degradation and dynamic instability more realistically. Time-dependent effects such as creep, shrinkage, and environmental influences were not included, though they can substantially modify stiffness evolution over a structure's service life. For future research, it is recommended to (i) extend the analysis to 3D RC frame–wall or core–slab systems, (ii) perform nonlinear time-history simulations with recorded ground motions to evaluate post-yield resilience, (iii) integrate experimentally calibrated crack-propagation and damage models for improved representation of stiffness loss, and (iv) develop a height-based stiffness degradation framework to support performance-based seismic design. The establishment of a library of effective stiffness coefficients, tailored to building height, geometric proportions, and loading conditions, will enhance the accuracy and efficiency of nonlinear seismic assessment in engineering practice.

5. Declarations

5.1. Author Contributions

Conceptualization, P.A.H.P.; methodology, P.A.H.P.; software, P.A.H.P. and N.H.N.; validation, P.A.H.P.; formal analysis, P.A.H.P. and N.H.N.; investigation, P.A.H.P.; resources, T.P.N. and N.H.N.; data curation, T.P.N. and N.H.N.; writing—original draft preparation, P.A.H.P., T.P.N., and N.H.N.; writing—review and editing, P.A.H.P. and T.P.N.; visualization, P.A.H.P., T.P.N., and N.H.N.; supervision, P.A.H.P.; project administration, P.A.H.P. All authors have read and agreed to the published version of the manuscript.

5.2. Data Availability Statement

The data presented in this study are available on request from the corresponding author.

5.3. Funding

The authors received no financial support for the research, authorship, and/or publication of this article.

5.4. Conflicts of Interest

The authors declare no conflict of interest.

6. References

[1] Tran, T.-H. (2025). Energy Dissipation and Stiffness Assessment: A Study on RC Frame Joints Reinforced with UHPSFRC. Structural Durability & Health Monitoring, 19(4), 869–886. doi:10.32604/sdhm.2025.064902.

[2] Galatage, A. A., & Patil, S. B. (2025). Seismic Assessment of First and Second Secant Stiffness for the Masonry Infilled RC Frame. Civil Engineering Journal (Iran), 11(2), 472–487. doi:10.28991/CEJ-2025-011-02-05.

[3] Pham, P. A. H., Le, C. V., & Nguyen, V. T. (2025). Effect of Infill Wall Opening Ratio on the Mechanical Characteristics of Reinforced Concrete Frames. Civil Engineering Journal (Iran), 11(8), 3454–3472. doi:10.28991/CEJ-2025-011-08-020.

[4] Paulay, T., & Priestly, M. J. N. (1992). Seismic Design of Reinforced Concrete and Masonry Buildings. John Wiley & Sons, Hoboken, United States. doi:10.1002/9780470172841.

[5] Pham, P. A. H., & Hung, C. C. (2024). An Approach for Plastic Hinge Length of RC Columns. Recent Advances in Structural Health Monitoring and Engineering Structures, SHM&ES 2023. Lecture Notes in Civil Engineering, 460, Springer, Singapore. doi:10.1007/978-981-97-0399-9_5.

[6] TCVN 9386:2012. (2012). Design of structures for earthquake resistance. Construction Publishing House, Hanoi, Vietnam. (In Vietnamese).

[7] ASCE/SEI 41-23. (2023). Seismic Evaluation and Retrofit of Existing Buildings. American Society of Civil Engineers (ASCE), Reston, United States. doi:10.1061/9780784416112.

[8] ACI Committee 318. (2025). Building Code for Structural Concrete—Code Requirements and Commentary. American Concrete Institute (ACI), Farmington Hills, United States.

[9] Hopkins, D. C. (1992). Seismic design of reinforced concrete and masonry buildings. Bulletin of the New Zealand Society for Earthquake Engineering, 25(4), 362. doi:10.5459/bnzsee.25.4.362.

[10] Elwood, K. J., & Eberhard, M. O. (2009). Effective Stiffness of Reinforced Concrete Columns. ACI Structural Journal, 106(4). doi:10.14359/56613.

[11] Ngoc Tran, C. T., & Li, B. (2012). Initial stiffness of reinforced concrete columns with moderate aspect ratios. Advances in Structural Engineering, 15(2), 265–276. doi:10.1260/1369-4332.15.2.265.

[12] Anh Huy, P. P., Yuen, T. Y., Hung, C. C., & Mosalam, K. M. (2022). Seismic behaviour of full-scale lightly reinforced concrete columns under high axial loads. Journal of Building Engineering, 56, 104817. doi:10.1016/j.jobe.2022.104817.

[13] Pham, H. P. (2023). Shear strength model of large-scale reinforced concrete rectangular columns with light transverse reinforcement. Asian Journal of Civil Engineering, 24(1), 219–244. doi:10.1007/s42107-022-00499-9.

[14] Gesualdi, G., Viggiani, L. R. S., & Cardone, D. (2020). Seismic performance of RC frame buildings accounting for the out-of-plane behavior of masonry infills. Bulletin of Earthquake Engineering, 18(11), 5343–5381. doi:10.1007/s10518-020-00904-1.

[15] Dong, G., Garcia, R., Pilakoutas, K., & Hajirasouliha, I. (2024). A review of optimum seismic design of RC frames: State-of-the-art, challenges and future directions. Engineering Structures, 315, 118455. doi:10.1016/j.engstruct.2024.118455.

[16] Liu, W., Givens, J. D., Kanitkar, R., & Blaney, C. (2009). Seismic Evaluation and Rehabilitation of a Three Story Pre-Northridge Steel Frame Essential Service Facility. Improving the Seismic Performance of Existing Buildings and Other Structures, 56–67. doi:10.1061/41084(364)6.

[17] Mazzoni, S., McKenna, F., Scott, M. H., & Fenves, G. L. (2006). OpenSees command language manual. Open System for Earthquake Engineering Simulation (OpenSees), Pacific earthquake engineering research (PEER) center, University of California, Berkeley, United States.

[18] Raja, D., & Rani, N. (2023). Analysis of progressive collapse of building using ETABS. Materials Today: Proceedings, 93, 278–286. doi:10.1016/j.matpr.2023.07.257.

[19] Computers and Structures Inc. (2016). Implemented E. SAP2000® Version 19.0. 0 Release Notes 2016. Computers and Structures Inc., California, United States.

[20] Khoshraftar, A., & Abbasnia, R. (2010). The effect of degradation on seismic damage of RC buildings. The International Conference on Civil and Architecture Engineering, 8(8), 1–11. doi:10.21608/iccae.2010.44423.

[21] Kumar, R., & Singh, Y. (2010). Stiffness of reinforced concrete frame members for seismic analysis. ACI Structural Journal, 107(5), 607–615. doi:10.14359/51663914.

[22] Lima, C., Martinelli, E., Macorini, L., & Izzuddin, B. A. (2017). Modelling beam-to-column joints in seismic analysis of RC frames. Earthquake and Structures, 12(1), 119–133. doi:10.12989/eas.2017.12.1.119.

[23] Guo, Z., Zhang, Y., Lu, J., & Fan, J. (2016). Stiffness degradation-based damage model for RC members and structures using fiber-beam elements. Earthquake Engineering and Engineering Vibration, 15(4), 697–714. doi:10.1007/s11803-016-0359-4.

[24] Hamidia, M., Afzali, M., Jamshidian, S., & Safi, M. (2023). Post-earthquake stiffness loss estimation for reinforced concrete columns using fractal analysis of crack patterns. Structural Concrete, 24(3), 3933–3951. doi:10.1002/suco.202200351.

[25] Loh, C. H., Mao, C. H., Huang, J. R., & Pan, T. C. (2011). System identification and damage evaluation of degrading hysteresis of reinforced concrete frames. Earthquake Engineering and Structural Dynamics, 40(6), 623–640. doi:10.1002/eqe.1051.

[26] Hung, C. C., Pham, P. A. H., Yuen, T. Y., & Mosalam, K. M. (2024). Full-scale cyclic testing of slender RC columns bent in double curvature under high axial load. Journal of Building Engineering, 82(108186). doi:10.1016/j.jobe.2023.108186.

[27] Di Sarno, L., & Amiri, S. (2019). Period elongation of deteriorating structures under mainshock-aftershock sequences. Engineering Structures, 196(109341). doi:10.1016/j.engstruct.2019.109341.

Appendix I

Table A1. Effective stiffness calculations according to design codes and proposed models

Specimens	L (mm)	b (mm)	h (mm)	f'_c (MPa)	E_b (MPa)	Axial force/Axial load ratio	TCVN 9386:2012 [6]	ACI 318 -25 [8]	Paulay & Priestley [9]	Tran & Li [11]	Elwood & Eberhard [10]	Test	(8)/(13)	(9)/(13)	(10)/(13)	(11)/(13)	(12)/(13)
(1)	(2)	(3)	(4)	(5)	(6)	(7)	(8)	(9)	(10)	(11)	(12)	(13)					
A-0.5P [26]	3000	400	400	49.7	33367	3978/0.5	15.8	22.1	19.0	18.3	22.4	28.7	0.55	0.77	0.66	0.64	0.78
B-0.5P [26]	3000	400	400	49.7	33367	3978/0.5	15.8	22.1	19.0	18.3	22.4	30.0	0.53	0.74	0.63	0.61	0.75
C-0.5P [26]	3000	400	400	49.7	33367	39780.5	15.8	22.1	19.0	18.3	22.4	27.4	0.58	0.81	0.69	0.67	0.82
C-F-H [12]	3200	800	800	43.5	31216	14822/0.53	195.1	273.1	312.2	137.9	217.2	117.3	1.66	2.33	2.66	1.18	1.85
C-FS-H [12]	3200	800	800	43.8	31324	14822/0.53	195.8	274.1	313.2	137.7	216.8	139.0	1.41	1.97	2.25	0.99	1.56
C-S-H [12]	3200	800	800	39.7	29822	14822/0.58	186.4	260.9	298.2	140.8	222.3	119.9	1.55	2.18	2.49	1.17	1.85
												Mean	1.30	1.82	2.02	1.00	1.52
												COV	0.32	0.32	0.37	0.21	0.27
C-0.1P [26]	3000	400	400	51.9	34097	830/0.1	16.2	9.7	12.9	10.3	9.4	14.7	1.10	0.66	0.88	0.70	0.64
C-F-L [12]	3200	800	800	42.5	30855	2560/0.09	192.8	115.7	154.3	71.2	82.6	77.8	2.48	1.49	1.98	0.92	1.06
C-FS-L [12]	3200	800	800	42.8	30964	2560/0.09	193.5	116.1	154.8	71.4	82.7	62.9	3.08	1.85	2.46	1.14	1.31
C-S-L [12]	3200	800	800	42.8	30964	2560/0.09	193.5	116.1	154.8	71.4	82.7	85.4	2.27	1.36	1.81	0.84	0.97
												Mean	2.23	1.34	1.78	0.90	1.00
												COV	0.32	0.32	0.32	0.18	0.24

Table A2. Comparison of stiffness prediction models

Method	Accuracy for high axial load ratio	Accuracy for low axial load ratio	Safety level in prediction	Stability (COV)
TCVN 9386:2012 [6]	Good	Poor (overestimated)	High	Moderate
ACI 318-25 [8]	Fair	Fair	Moderate	Moderate
Paulay & Priestley [9]	Slightly conservative	Slightly conservative	High	High variation
Tran & Li [11]	Most accurate	Most accurate	Balanced	Best
Elwood & Eberhard [10]	Good	Good	Slightly conservative	Good